

Title	Photoluminescence, morphology, and structure of hydrothermal ZnO implanted at room temperature with 60 keV Sn ⁺ ions
Author(s)	Dang, Giang T.; Kawaharamura, Toshiyuki; Nitta, Noriko; Hirao, Takashi; Yoshiie, Toshimasa; Taniwaki, Masafumi
Citation	JOURNAL OF APPLIED PHYSICS (2011), 109(12)
Issue Date	2011-06
URL	http://hdl.handle.net/2433/160650
Right	Copyright 2011 American Institute of Physics. This article may be downloaded for personal use only. Any other use requires prior permission of the author and the American Institute of Physics. The following article appeared in JOURNAL OF APPLIED PHYSICS 109, 123516 (2011) and may be found at http://link.aip.org/link/?jap/109/123516
Type	Journal Article
Textversion	publisher

Photoluminescence, morphology, and structure of hydrothermal ZnO implanted at room temperature with 60 keV Sn⁺ ions

Giang T. Dang, Toshiyuki Kawaharamura, Noriko Nitta, Takashi Hirao, Toshimasa Yoshiie et al.

Citation: *J. Appl. Phys.* **109**, 123516 (2011); doi: 10.1063/1.3598068

View online: <http://dx.doi.org/10.1063/1.3598068>

View Table of Contents: <http://jap.aip.org/resource/1/JAPIAU/v109/i12>

Published by the [American Institute of Physics](#).

Related Articles

ZnO/ZnS_xSe_{1-x} core/shell nanowire arrays as photoelectrodes with efficient visible light absorption
Appl. Phys. Lett. **101**, 073105 (2012)

Study of the photoluminescence emission line at 3.33eV in ZnO films
J. Appl. Phys. **112**, 013528 (2012)

Correlation of spectral features of photoluminescence with residual native defects of ZnO thin films annealed at different temperatures
J. Appl. Phys. **112**, 013525 (2012)

Optical analysis of doped ZnO thin films using nonparabolic conduction-band parameters
J. Appl. Phys. **111**, 123507 (2012)

Structural transition in II-VI nanofilms: Effect of molar ratio on structural, morphological, and optical properties
J. Appl. Phys. **111**, 113510 (2012)

Additional information on J. Appl. Phys.


Journal Homepage: <http://jap.aip.org/>

Journal Information: http://jap.aip.org/about/about_the_journal

Top downloads: http://jap.aip.org/features/most_downloaded

Information for Authors: <http://jap.aip.org/authors>

ADVERTISEMENT



AIP Advances

Special Topic Section:
PHYSICS OF CANCER

Why cancer? Why physics? [View Articles Now](#)

Photoluminescence, morphology, and structure of hydrothermal ZnO implanted at room temperature with 60 keV Sn⁺ ions

Giang T. Dang,^{1,a)} Toshiyuki Kawaharamura,² Noriko Nitta,² Takashi Hirao,² Toshimasa Yoshiie,³ and Masafumi Taniwaki¹

¹*Department of Environmental Systems Engineering, Kochi University of Technology, Kami, Kochi 782-8502, Japan*

²*Research Institute for Nano-devices, Kochi University of Technology, Kami, Kochi 782-8502, Japan*

³*Research Reactor Institute, Kyoto University, Kumatori-cho, Osaka 596-0821, Japan*

(Received 29 March 2011; accepted 10 May 2011; published online 21 June 2011)

Hydrothermal ZnO wafers implanted at room temperature with 60 keV Sn⁺ ions are examined by means of photoluminescence (PL), atomic force spectroscopy (AFM), and X-ray diffractometry techniques. The PL intensity significantly decreases in the wafers implanted to doses of 4.1×10^{13} ions/cm² and higher. The AFM measurements indicate that surface roughness variation is not the cause of the significant decrease in PL intensity. Furthermore, the PL deep level (DL) band peak blueshifts after illuminating the implanted samples with the He-Cd laser 325 nm line; meanwhile, the DL band intensity first increases and then decreases with illumination time. These abnormal behaviors of the DL band are discussed. © 2011 American Institute of Physics. [doi:10.1063/1.3598068]

I. INTRODUCTION

ZnO attracted extensive research attention in the middle of the 20th century,¹ and has recently been of renewed interest due to developments in growth technique² and great concern about (opto)electronics devices working in the blue and violet regions.³ Due to its large excitonic binding energy of 60 meV, ZnO is a promising material for excitonic lasing even at room temperature (RT).⁴ However, several problems still remain in the study of ZnO, for instance, the origin of various defects responsible for deep level (DL) photoluminescence (PL) band ranging from green to yellow-orange regions (500–600 nm).^{5–10}

The PL band mentioned above is relatively broad and highly asymmetric, indicating that numerous transitions of close energy contribute to it. Clearly, for the identification of the origins of those transitions it is necessary to first vary the conditions, which can cause changes in position and/or intensity of the band, and then analyze why those changes occur. Several methods have been applied, for example, using different growth techniques and varying parameters during the growth processes,^{7–9} and annealing ZnO in different atmospheres.^{6,10} As an alternative, the implantation technique has been widely employed to vary optical and electronic properties, structure, and morphology of materials.^{11–16} In this study, we implanted ZnO at RT with 60 keV Sn⁺ ions to numerous doses. PL of the implanted samples was measured. Atomic force microscopy (AFM) and X-ray diffractometry (XRD) measurements were employed to examine the morphology and structure of the samples. In addition, this study reports the effect of illumination with the 325 nm line of a He-Cd laser on the DL band PL.

II. EXPERIMENT

ZnO (99.99%) wafers 0.54 mm thick were grown by the hydrothermal method. The zinc surface of the (0001) plane of these wafers was implanted at RT with 60 keV Sn⁺ ions to doses of 3.6×10^{12} , 4.1×10^{13} , 8.0×10^{13} , 1.6×10^{14} , and 2.5×10^{14} ions/cm². These wafers are hereafter referred to by their implantation doses, for example, the 2.5×10^{14} sample.

In the PL measurements, the samples were excited with the 325 nm line of a He-Cd laser; the excitation power was 12 W/cm². The PL emission was focused on the slit of a 0.32 m diffraction-grating spectrometer (iHR320 HOBIRA Jobin Yvon), and a 256×1024 pixel charge coupled device (CCD) array (the Synapse CCD camera HOBIRA Jobin Yvon) was used to record the PL spectra. The samples were also illuminated with the same 325 nm He-Cd laser line; the illumination power was 60 W/cm². Morphology of the samples was investigated by means of a JEOL TM-4210BU Scanning Probe Microscope, which was set to the AFM contact mode. XRD patterns were measured by means of an ATX Rigaku XRD-diffractometer using the Cu K α line ($\lambda = 1.5418$ Å). All measurements were conducted at RT.

III. RESULTS

Figures 1(a) and 1(b) plot the XRD 0002 and 0004 reflections of the samples. In both figures, a low-angle shoulder appeared in the samples implanted to doses of 4.1×10^{13} ions/cm² and higher and it moved further in the low-angle direction as the implantation dose was increased. This indicates the presence of a strain profile resulting from a large number of point defects, point defect complexes, or even dislocations and dislocation loops.^{14–16}

Previously, we reported¹⁷ the PL spectra of a batch of ZnO wafers implanted with 60 keV Sn⁺ ions to doses of

^{a)}Author to whom correspondence should be addressed. Electronic mail: 128007t@gs.kochi-tech.ac.jp.

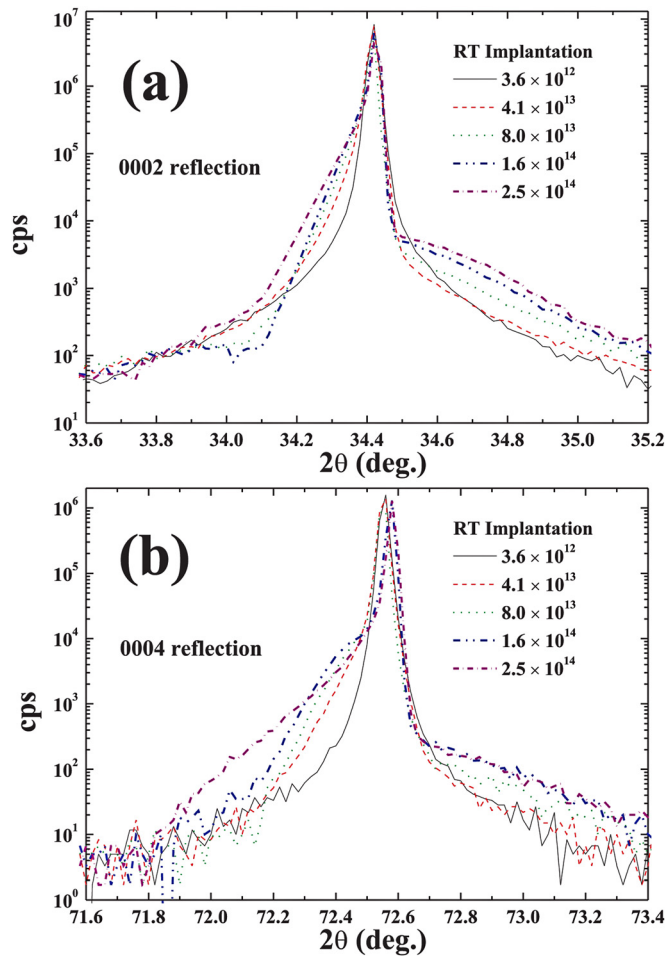


FIG. 1. (Color online) XRD detailed scans around the (a) 0002, (b) 0004 reflections.

$4 - 15 \times 10^{14}$ ions/cm². In the current batch of samples, implantation dose was intentionally reduced ($3.6 \times 10^{12} - 2.5 \times 10^{14}$ ions/cm²) to obtain more intense photoemission. PL spectra of these low-dose samples are depicted in Fig. 2. Note that the unimplanted ZnO PL spectrum was measured in the unimplanted area on the surface of

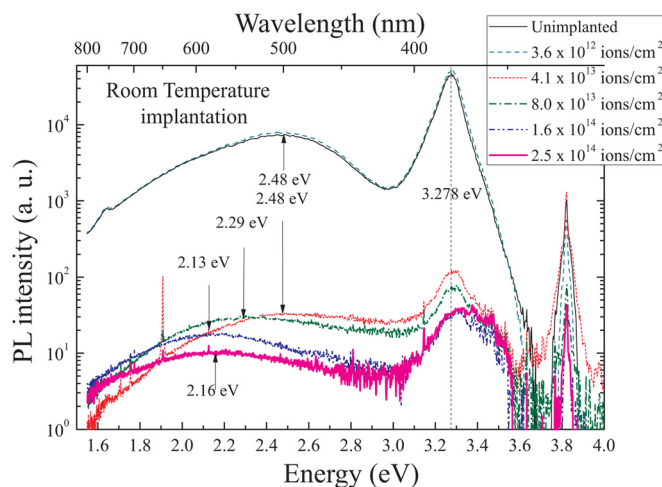


FIG. 2. (Color online) PL spectra of ZnO wafers implanted at RT with 60 keV Sn⁺ to various doses.

the 3.6×10^{12} sample. As can be seen, two regions appeared in the unimplanted ZnO PL spectrum: the near-band-edge (NBE) region peaking at 3.278 eV (378 nm) and the deep level (DL) region peaking at 2.48 eV (500 nm). The DL peak position of the current batch differed slightly from that of the previous batch (521 nm),¹⁷ probably because of difference in relative concentrations of various existing point defects. This reason was mentioned in the study of Børseth *et al.*⁶ At an implantation dose as low as 3.6×10^{12} ions/cm², the ZnO wafer remained intact, which was evident in the similarity of the PL spectra of the unimplanted and implanted areas. However, when the implantation dose was increased to 4.1×10^{13} ions/cm², the PL intensity decreased significantly, by more than two orders of magnitude. This casts doubt on the previous claim that a high level of dynamic annealing makes ZnO highly resistant to implantation-induced damages.¹² A further increase in implantation dose caused a gradual decrease in PL intensity of both NBE and DL regions. In addition, the DL region peak redshifted with implantation dose; this effect was essentially the same as that reported previously in hydrothermal ZnO irradiated with 4 MeV electrons.⁷ According to Ref. 7, electron irradiation could not introduce new impurity-related defects but the redshift still occurred; similarly, in the current study most likely Sn⁺-related defects did not cause the redshift of the DL band.

To verify whether morphology changes during implantation were responsible for the abrupt decrease in PL of the ZnO wafers implanted to the doses of 4.1×10^{13} ions/cm² and higher, AFM measurements were conducted. Figures 3(a)–3(e) show the AFM images of all the ZnO wafers. As can be seen in these figures, no significant variations in morphology were observed. In each image, root mean square (RMS) roughness of five approximately 200 nm long lines was calculated. These lines were selected so that they did not cross scratches on the sample surface, as shown by arrows in Figs. 3(a)–3(e). Each sample was imaged at various imaging parameters, and the RMS roughness was averaged overall recorded images. It should be noted that the calculation procedure was essentially the same for all samples. The calculated RMS roughness is plotted in Fig. 3(f) as a function of implantation dose. As can be seen in the figure, the RMS roughness of the wafers implanted to doses of 3.6×10^{12} , 4.1×10^{13} , 8×10^{13} , and 1.6×10^{14} ions/cm² was just slightly different, whereas the PL intensity of the 3.6×10^{12} sample was by more than two orders of magnitude larger than that of the other samples (see Fig. 2). The AFM measurements indicate that surface variation was not the main reason for the abrupt decrease in PL intensity.

In Fig. 4, the effect of illumination on PL behaviors of the ZnO wafers is demonstrated. The samples were illuminated with 60 W/cm² laser (the same 325 nm He-Cd laser line) for numerous illumination times. Shown in Fig. 4(a) are the PL spectra of the 1.6×10^{14} sample after 0, 10, 160, and 2560 s illumination. As can be observed, as illumination time was increased, the NBE peak remained almost unchanged. Meanwhile, the DL peak blueshifted and the DL band intensity first increased and then steadily decreased with illumination time; note that all these variations were

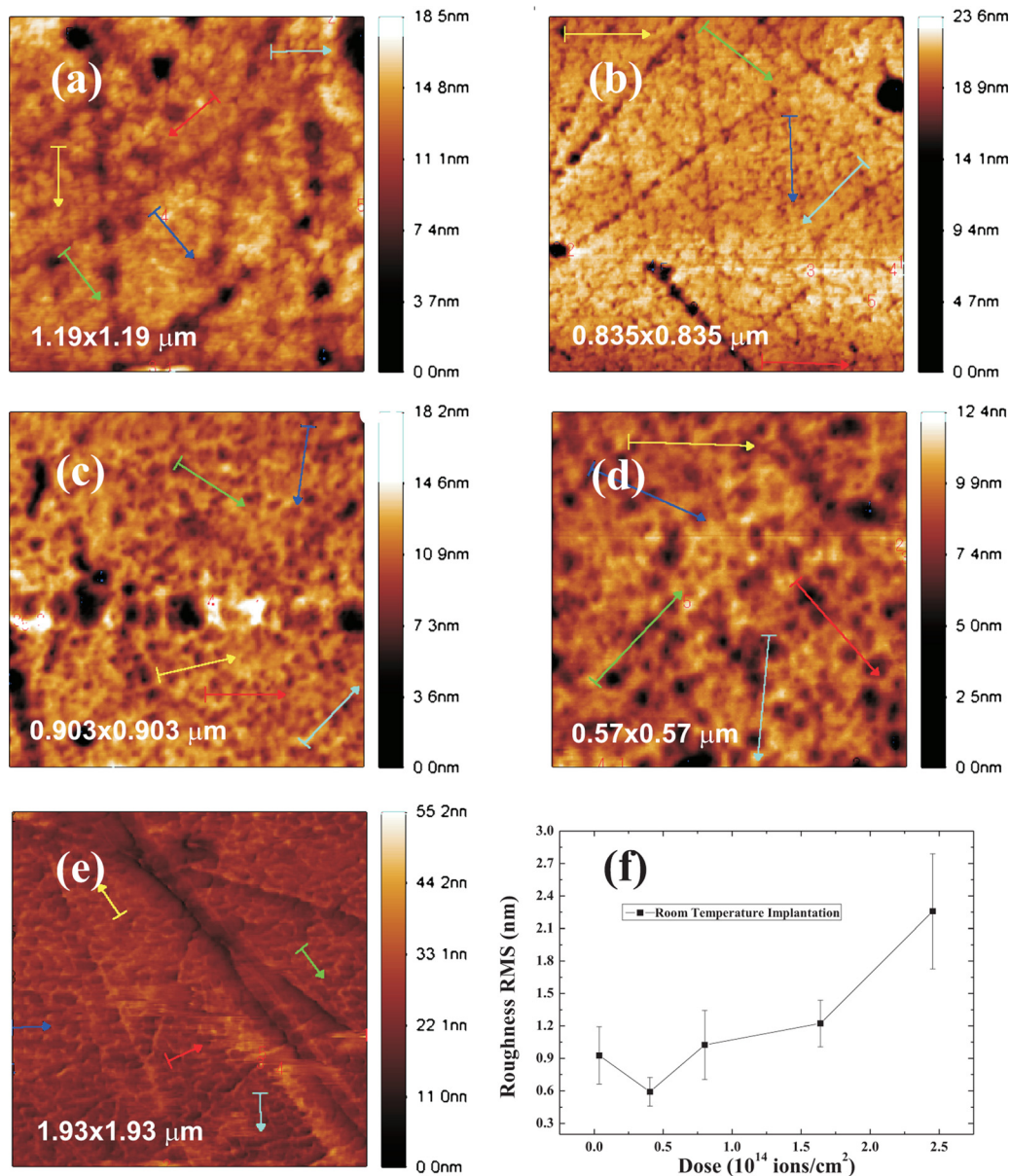


FIG. 3. (Color online) AFM images of ZnO wafers implanted to doses of (a) 3.6×10^{12} , (b) 4.1×10^{13} , (c) 8.0×10^{13} , (d) 1.6×10^{14} , and (e) 2.5×10^{14} ions/cm² (f) implantation dose dependence of RMS roughness.

irreversible. The observations are quantitatively detailed in Fig. 4(b). The integrated PL intensities of the NBE and DL regions were normalized by the maximum integrated PL intensity and then were depicted as functions of illumination time, along with the DL band peak position. The DL band intensities of the 8.0×10^{13} and 2.5×10^{14} samples behaved in the same manner as the 1.6×10^{14} sample upon increase in illumination time; namely, an initial growth was followed by a steady decrease. This was evident in Fig. 4(c). The inset in Fig. 4(c) also shows that the initial growth stage lasted for a shorter time as the implantation dose was decreased. In particular, in the 4.1×10^{13} sample the initial growth of PL intensity did not occur. The data indicate that implantation-induced defects, which resulted in the redshift of the DL band, were eliminated by illumination with the He-Cd laser 325 nm line; consequently, the band blueshifted.

IV. DISCUSSION

Previously, Singh *et al.*¹⁸ have reported RMS roughness of 0.7 nm in the “un-exfoliated” area of ZnO implanted with 100 keV H_2^+ ions to a dose of 2.7×10^{17} ions/cm². In addition, Coleman *et al.*¹¹ have reported RMS roughness of ZnO single crystal implanted at RT with 300 keV As^+ ions to a dose of 1.4×10^{17} ions/cm² and that of unimplanted ZnO to be 2.5 nm and 0.6 nm, respectively. These values are in the same order of magnitude as the RMS roughnesses of the 2.5×10^{14} (2.3 nm) and 3.6×10^{12} (0.9 nm) samples in the current study. It appears that RMS roughness did increase with implantation dose; however, the increase was not the cause of the significant decrease in PL intensity. The PL decrease was probably caused by implantation-induced non-radiative defects inside the implanted layer rather than on the surface.

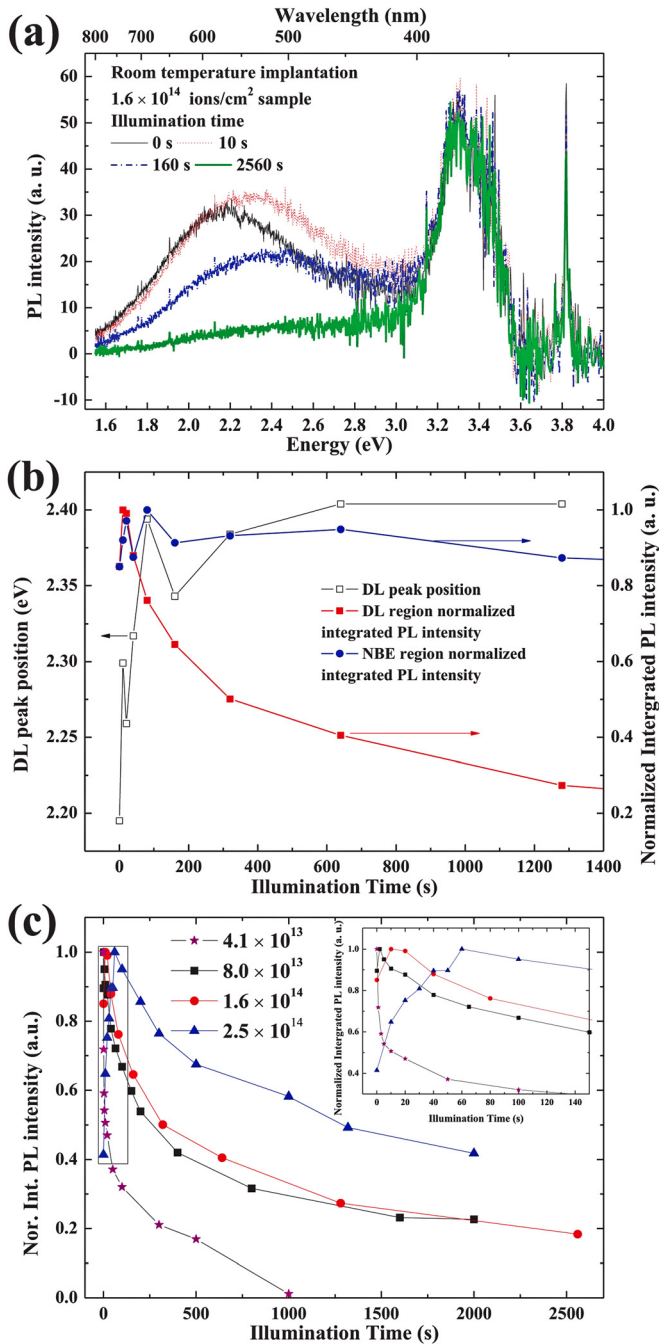


FIG. 4. (Color online) (a) PL spectra of the 1.6×10^{14} ions/cm² sample illuminated with the 325 nm line of a He-Cd laser after 0, 10, 160, and 2560 seconds; (b) illumination time dependences of the DL peak position, DL and NBE band integrated PL intensities in the 1.6×10^{14} ions/cm² sample; (c) illumination time dependences of the DL integrated intensity in the 4.1×10^{13} , 8.0×10^{13} , 1.6×10^{14} , and 2.5×10^{14} samples; the inset shows the detailed view of the area hedged by the rectangle.

Recently, Evans *et al.*¹⁹ and Laiho *et al.*²⁰ have independently reported the dependence of electron paramagnetic resonance (EPR) intensity of singly ionized oxygen vacancies V_O^+ on illumination time. This dependence was surprisingly similar to that of the DL band PL intensity in the current study; namely, initial rapid growth was followed by a steady decrease. Meanwhile, it has been illustrated that the DL band peaked at 2.15, 2.37, and 2.55 eV as hydrothermal

ZnO was annealed in ZnO, O-rich, and Zn-rich atmospheres, respectively.⁶ In addition, the 2.37 and 2.55 peaks could be easily switched by solely varying annealing atmospheres.⁶ Børseth *et al.*⁶ attributed the 2.15, 2.37, and 2.55 bands to Li-related, V_{Zn} , and V_O point defects, respectively. In another study, Studenikin *et al.*⁸ have also claimed that annealing in oxygen-deficient atmospheres resulted in the green band emission (2.43 eV), while annealing in oxygen-rich atmospheres resulted in red band emission (1.94 eV). Furthermore, Zhao *et al.*¹⁰ have attributed the band peaking at 2.38 eV to V_{Zn} , based on the fact that Zn implants exerted more influence over the PL intensity than O implants. On the basis of the studies mentioned above, we discuss the abnormal variations of the DL band with implantation dose and illumination time, as follows.

Following the assignment of Zhao *et al.*,¹⁰ suppose that the green emission was due to the Zn-related defect transition (we presume that it is the $Zn_i \rightarrow V_{Zn}^-$ transition).¹⁷ Implantation introduced more V_O point defects (V_O^\times , V_O^+ , and V_O^{++}), which facilitated the conduction band to V_O^+ transition ($CB \rightarrow V_O^+$) in the orange region; therefore, the DL band redshifted with implantation dose. During illumination, a V_O^\times center released an electron,^{19,21} thus, the V_O^+ concentration initially increased; further illumination reduced the V_O^+ concentration via the hole trapping reaction $V_O^+ + h \rightarrow V_O^{++}$.²¹ This explains the variation of the DL band PL intensity with illumination time and, partly, the blueshift after long time exposure. However, the model could not explain why the DL band blueshifted after short time exposure when the increase in V_O^+ concentration still occurred. The model would contradict the studies of Børseth *et al.*⁶ and Studenikin *et al.*⁸

On the contrary, following the assignment of Børseth *et al.*,⁶ suppose that the green band was due to a V_O -related transition (we presume that the oxygen vacancy is V_O^+ in this case); there are two scenarios here. First, implantation with Sn^+ ions reduced the relative V_O^+ concentration in comparison with that of other defects. According to Børseth *et al.*,⁶ the redshift with implantation dose could be attributed to the Li-related defect, for which the relative concentration became dominant. Furthermore, illumination recovered the relative V_O^+ concentration via the electron-releasing mechanism (see the previous paragraph) as evident in the initial growth in the DL band PL intensity, and the band blueshifted. Second, implantation increased the V_O^+ concentration. As indicated by the XRD data (see Fig. 1), formation of complexes such as multi-vacancies, multi-interstitials, or even dislocations occurred, including V_O^+ -complexes. Furthermore, the DL band redshifted with implantation dose because either (1) the V_O^+ -complexes were still radiative and their energy was smaller than the energy of individual point defects, as argued by Studenikin *et al.*⁸; or (2) the complexes were non-radiative and emission from Li-related defects became dominant, as argued by Børseth *et al.*⁶ During illumination, the complexes dissociated and the number of individual point defects increased, which in turn caused the DL band blueshift and an initial PL intensity increase. However, it is unclear which mechanism accounted for the dissociation of the complexes, given a small variation in temperature during illumination. Moreover, both scenarios could not

naturally explain the next stage when the DL band continued blueshifting as the band intensity decreased.

Clearly, more investigations are necessary to satisfactorily explain the abnormal behaviors of the DL band.

V. CONCLUSION

Hydrothermal ZnO wafers were implanted at RT with 60 keV Sn⁺ ions to doses of 3.6×10^{12} , 4.1×10^{13} , 8.0×10^{13} , 1.6×10^{14} , and 2.5×10^{14} ions/cm². These wafers were examined by photoluminescence (PL), atomic force spectroscopy (AFM), and X-ray diffractometry (XRD) techniques. The PL intensity significantly decreased in the wafers implanted to the doses of 4.1×10^{13} ions/cm² and higher. The AFM measurements indicated that the roughness variation was not the cause of the significant decrease in PL intensity. Furthermore, under illumination of the He-Cd laser 325 nm line the DL band peak in the PL spectra of the implanted samples blueshifted, and the DL band intensity first increased and then steadily decreased with illumination time. The illumination time dependence of PL intensity was similar to the dependence of EPR V_O⁺ signal reported previously.^{19,20} The abnormal behaviors of the DL band were discussed.

¹F. A. Kroger and H. J. Vink, *J. Chem. Phys.* **22**, 250 (1954).

²Y. Chen, D. Bagnall, and T. Yao, *Mater. Sci. Eng. B* **75**, 190 (2000).

³C. Jagadish and S. J. Pearton, *Zinc Oxide Bulk, Thin Films and Nanostructures* (Elsevier, Oxford, 2006).

⁴Y. R. Ryu, J. A. Lubguban, T. S. Lee, H. W. White, T. S. Jeong, C. J. Youn, and B. J. Kim, *Appl. Phys. Lett.* **90**, 131115 (2007).

⁵Ü. Özgür, Y. I. Alivov, C. Liu, A. Teke, M. A. Reshchikov, S. Doğan, V. Avrutin, S.-J. Cho, and H. Morkoç, *J. Appl. Phys.* **98**, 041301 (2005).

⁶T. M. Børseth, B. G. Svensson, A. Y. Kuznetsov, P. Klason, Q. X. Zhao, and M. Willander, *Appl. Phys. Lett.* **89**, 262112 (2006).

⁷V. A. Nikitenko, *J. Appl. Spectrosc.* **57**, 783 (1992) [*Zh. Prikl. Spektrosk.* **57**, 367 (1992) (in Russian)].

⁸S. A. Studenikin, N. Golego, and M. Cocivera, *J. Appl. Phys.* **84**, 2287 (1998).

⁹M. Liu, A. H. Kitai, and P. Mascher, *J. Lumin.* **54**, 35 (1992).

¹⁰Q. X. Zhao, P. Klason, M. Willander, H. M. Zhong, W. Lu, and J. H. Yang, *Appl. Phys. Lett.* **87**, 211912 (2005).

¹¹V. A. Coleman, H. H. Tan, C. Jagadish, S. O. Kucheyev, and J. Zou, *Appl. Phys. Lett.* **87**, 231912 (2005).

¹²S. O. Kucheyev, J. S. Williams, C. Jagadish, J. Zou, C. Evans, A. J. Nelson, and A. V. Hamza, *Phys. Rev. B* **67**, 094115 (2003).

¹³N. Nitta, M. Taniwaki, Y. Hayashi, and T. Yoshiie, *J. Appl. Phys.* **92**, 1799 (2002).

¹⁴J. Cheng and F. B. Prinz, *Nucl. Instrum. Methods Phys. Rev. B* **227**, 577 (2005).

¹⁵P. Zaumseil, U. Winter, F. Cembali, M. Servidori, and Z. Sourek, *Phys. Status Solidi A* **100**, 95 (1987).

¹⁶H. Iwanaga, N. Shibata, K. Suzuki, and S. Takeuchi, *Philos. Mag.* **35**, 1213 (1977).

¹⁷G. T. Dang, T. Kawaharamura, T. Hirao, N. Nitta, and M. Taniwaki, *AIP Conf. Proc.* **1321**, 270 (2010).

¹⁸T. Singh, R. Scholz, S. H. Christiansen, U. Gösele, and R. Singh, *Phys. Status Solidi C* **7**, 444 (2010).

¹⁹S. M. Evans, N. C. Giles, L. E. Halliburton, and L. A. Kappers, *J. Appl. Phys.* **103**, 043710 (2008).

²⁰R. Laiho, L. S. Vlasenko, and M. P. Vlasenko, *J. Appl. Phys.* **103**, 123709 (2008).

²¹L. S. Vlasenko, *Physica B* **404**, 4774 (2009).